LAWRENCE
LIVERMORE
NATIONAL
LABORATORY

LLNL-JRNL-403680

Space-Time Characterization of Laser Plasma Interactions in the Warm Dense Matter Regime

L. F. Cao, I. Uschmann, E. Forster, F. Zamponi, T. Kampfer, A. Fuhrmann, A. Holl, R. Redmer, S. Toleikis, T. Tschentsher, S. H. Glenzer

May 8, 2008

Laser Particle Beams

Disclaimer

Space-Time Characterization of Laser Plasma Interactions in the Warm Dense Matter Regime [a]

L. F. Cao, I. Uschmann, E. Förster, F. Zamponi, T. Kämpfer, A. Fuhrmann,

Institute for Optics and Quantum Electronics, Friedrich-Schiller-University, Max-Wien-Platz 1, D-07743 Jena, Germany

A. Höll, R. Redmer,

Institute for Physics, University Rostock, Universitätsplatz 3, D-18051 Rostock, Germany

S. Toleikis,T. Tschentscher,

Hasylab, DESY Hamburg, Notkestraße 85, D-22603 Hamburg, Germany

S. H. Glenzer

L-399, Lawrence Livermore National Laboratory, University of California, P.O. Box 808, Livermore, CA 94551, USA

Abstract: Laser plasma interaction experiments have been performed using a fs Titanium Sapphire laser. Plasmas have been generated from planar PMMA targets using single laser pulses with 3.3 mJ pulse energy, 50 fs pulse duration at 800 nm wavelength. The electron density distributions of the plasmas in different delay times have been characterized by means of Nomarski Interferometry. Experimental data were compared with hydrodynamic simulation. First results to characterize the plasma density and temperature as a function of space and time are obtained. This work aims to generate plasmas in the warm dense matter (WDM) regime at near solid-density in an ultra-fast laser target interaction process.

[a] Email address: cao@ioq.uni-jena.de

Plasmas under these conditions can serve as targets to develop x-ray Thomson scattering as a plasma diagnostic tool, e.g., using the VUV free-electron laser (FLASH) at DESY Hamburg.

I. Introduction

Definite measurements of plasma temperatures and densities are important for understanding and modeling contemporary plasma experiments in the WDM regime [1], i.e. at electron densities of n_e=10^{21} – 10^{26} cm^{-3} and temperatures of several eV. Of special interest is WDM at near-solid density at n_e=10^{21} – 10^{22} cm^{-3} where the transition from an ideal plasma to a weakly degenerate, weakly coupled plasma occurs. Novel plasma diagnostic methods for WDM are currently developed like, for instance, x-rays Thomson scattering [2, 3]. This new technique has been boosted by inertial confinement fusion (ICF) studied using x-ray back lighters [4] and has successfully been demonstrated at solid density Be plasmas [5]. At near-solid density a proof of principle of Thomson scattering experiment is currently implemented at the VUV Free Electron Laser (FLASH) at DESY, Hamburg. The goal of these experiments is to verify a consistent many-particle theory which accounts for quantum effects as well as small and long range correlations [7-10]. Recently, the extension of Thomson scattering in nonequilibrium plasmas to probe transient plasma behavior is discussed [11]. The elaboration of plasma dynamics will be the focus of future plasma experiments at FLASH and elsewhere [12].

The creation of WDM is a longstanding issue. Natural sources to isochorically heat solid targets in a large volume are shock waves, high brilliant x-ray sources or heavy ion beams. At smaller scales, near-solid density plasmas can also be created in ultra-short high-intensity laser matter interaction. In such laser experiments the plasma density and temperature of plasma

ablated from a planar solid surface changes in time and depends on the space distance from the surface on the laser parameters. The aim of the current work is a detailed experimental characterization of such ablative plasmas from planar PMMA bulk material. For the plasma characterization a modified time-resolved Nomarski interferometer [13] supplemented by numeric simulations is applied. These are prerequisite studies for an implementation into a pump-probe scattering experiment using the FLASH facility as the probe option.

The paper is organized as follows. In section II we outline the experimental setup to create the plasma and present numerical results of hydrodynamic simulations of the laser target interaction using PMMA targets. The time-resolved Interferometry density measurement technique in pump-probe type experiments is presented in section III. Section IV gives the experimental results, describes the data analysis and compares with the numerical simulations. Section V concludes and gives a short outlook.

II. Numerical simulation of laser PMMA target interaction

Figure 1 shows the sketch illustrating the laser target interaction. An ultra-short pulse laser irradiates perpendicular on a planar PMMA target and ablative plasmas are generated and evolve in time. This evolution can be obtained from hydrodynamic simulations. We employ the one-dimensional hydrodynamic code MED 103 [14], which has successfully been applied in laser plasmas interaction studies [15-17]. As an input the details of the laser pulse, wavelength, energy, duration and pulse shape, as well as target properties, material, density and geometric configuration have to be provided. As a result of the simulation we obtain space-time dependent plasma parameters including plasma density, plasma temperature, ionization state, pressure, and plasma velocity. The time resolved plasma density distribution and the plasma temperature distribution are of special interest in the current studies.

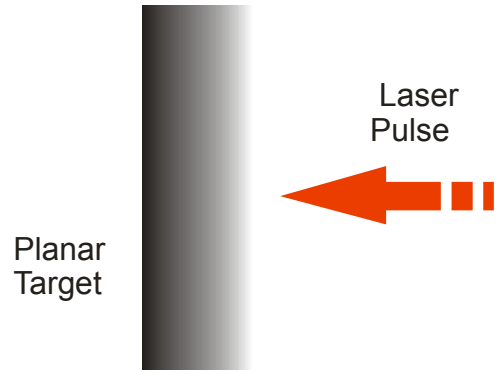

Figure 1 schematic for the calculation

Figure 2 shows results of the simulations for a Gaussian laser pulse at 800 nm wavelength, 50 fs pulse duration, and 5×10^{16} W/cm^2 intensity. The highest electron densities (n_e>7×10^{23} cm^{-3}) and temperatures (T_e>60 eV) are observed after the laser target interaction at the target surface. Subsequently, the plasma expands perpendicular to the target surface into the target as well as outwards. Therefore, as a function of the delay time after the pulse, the plasma volume grows and, consequently, the plasma density and temperature decreases. Whereas for short delay times the near-solid density region is only reached very close to the target surface with a steep spatial density gradient, at larger delay times the density gradients are more relaxed and the higher density region is expanded further outwards. The distance Δz_0 from the rear target side at which an electron density of 10^{21} cm^{-3} is observed runs from ~7 μm at 5 ps delay to ~40 μm at 300 ps time delay. The target thickness is d=5 μm. At the distance $\Delta z < \Delta z_0$ the plasma exists in the near-solid-density region.

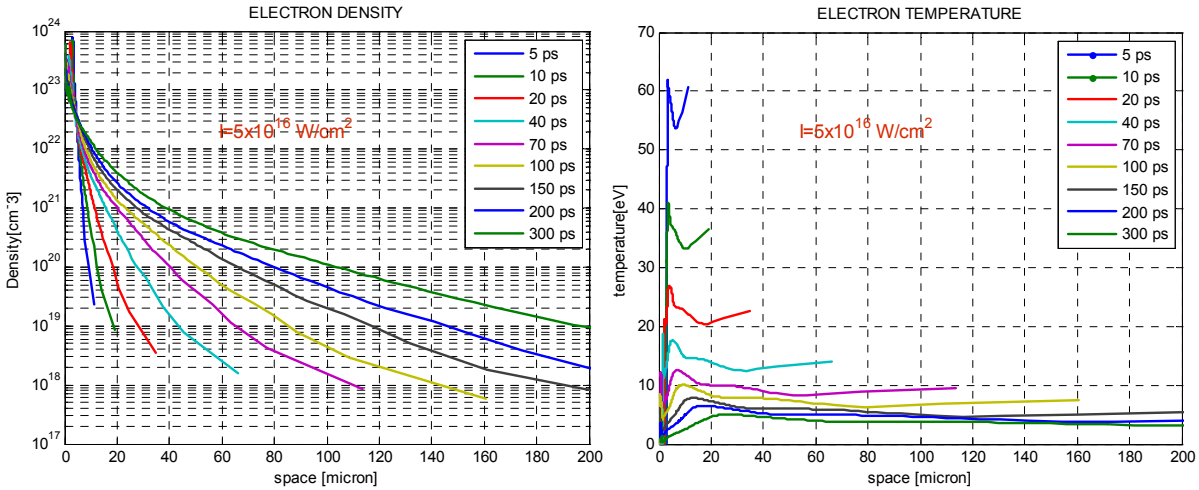

a b

Figure 2. 1-D Numerical simulation result for laser PMMA planar target interaction. As a function of the distance from the target surface it is shown a) the electron density profile; b) the electron temperature profile for different delay times. The laser intensity is 5×10^{16} W/cm^2.

Table 1. Dependence of the distance Δz_0 where a density of 10^{21} cm^{-3} is observed to the rear target side and the corresponding plasma temperature as a function of laser intensity and pulse duration. The pump-probe delay time is 300 ps.

Laser intensity I (W/cm^2)	Pulse duration τ (fs)	Distance to the target to limit the Region of the plasma at the density of 10^{21}~10^{22} cm^{-3} Δz_0 (μm)	Electron temperature of the warm dense matter T_e (eV)
10^{13}	100	(≤1) <6	<0.1
10^{14}	100	(<4) <9	<0.7
10^{15}	100	(<7) <12	<2
10^{16}	100	(<16) <21	<7
5×10^{16}	50	(<35) <40	<6

Further results showing the dependence of the distance Δz_0 on the laser intensity for a delay time and laser intensity of 300 ps are listed in Table 1. It is seen, that a plasma density

larger than 10^{21} cm^{-3} is produced only close to the target surface. Increasing laser intensity extends the region further away from the target to about 40 μm at an intensity of 10^{16} W/cm^2. This means that it is impractical to generate the warm dense matter by laser beam with less intensity than 10^{16} W/cm^2. Higher laser intensity than 5×10^{16} W/cm^2 might be more suitable, however, this goes beyond the capability of our Titanium Sapphire laser system.

III. Electron density measurement with optical laser interferometry

Optical laser interferometry [13, 18-23] had been verified a convenient, efficient and accurate technique to measure the electron density of plasma generated by short pulse laser. But the capability is limited by two factors: the first one is the critical density and the second is due to the deflection of the probe light in plasma with gradient density [24, 25]. Plasma densities higher than 1.7×10^{20} cm^{-3} had not been measured using optical laser interferometry. The deflection of light due to electron density gradients reduce the observation limit for optical laser interferometry further below the critical density and, therefore, WDM is not directly accessible.

However, an extrapolation from the low density region which is experimentally accessible to the high density region (see Figure 2-a) can provide an indication to characterize the WDM region. In this work, we measure the electron density profile at lower densities ($<2\times10^{20}$ cm^{-3}) and estimate the WDM region by extrapolation.

The setup of our pump-probe interferometry experiment is shown in Figure 3. A single laser pulse with wavelength of 800 nm, pulse duration 50 fs and pulse energy of 3.3 mJ is delivered to an unbalance beam splitter. 99% of the beam energy is reflected to a mirror M5 and then focused by a parabola onto the planar PMMA target. A focal size of diameter d~10-15μm at the target surface has been measured. Hence, the laser intensity reached is about 5×10^{16} W/cm^2. The other 1% part of the beam was frequency doubled by a BBO, subsequently sent through a

time delay line composed of the mirrors M1 and M2, and finally reflected to the plasma by the mirrors M3 and M4. The imaging system to observe the ablated plasma is composed of a microscope with a magnification of 10, Lens 1 and Lens 2, and an optical CCD. A Nomarski interferometer with intended modification (Figure 4) is obtained by additionally including a Wollaston prism and an additional polarizer.

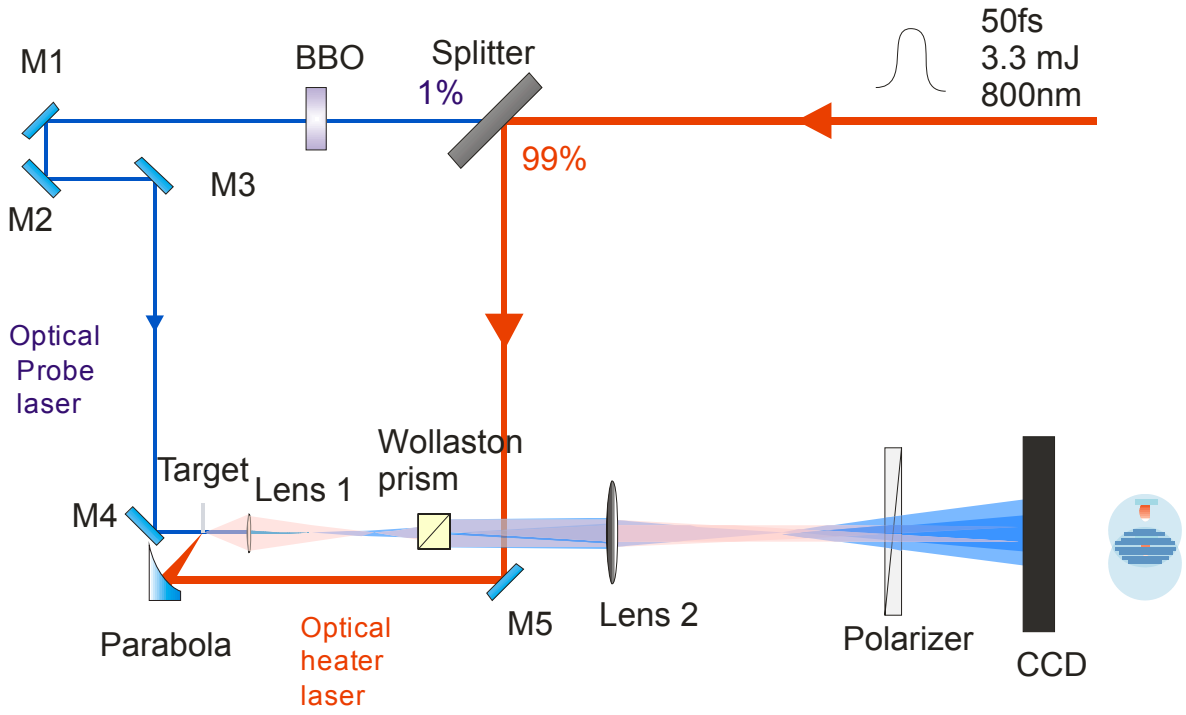

Figure 3. Setup of the laser plasma interferometry experiments.

The probe laser, including a portion distorted by the plasma, is split by the Wollaston prism into two beams with perpendicular polarization directions and two images appear on the CCD. The 45º polarizer projects the two perpendicular polarizations onto a single polarization direction and due to the relative phase shift between the plasma distorted light and the undistorted light an interference pattern appears on the CCD. Note that the interferometer used here differs slightly from the one formerly used [13]. The modified interferometer can collect deflected light with a

larger deflection angle, and hence, can reach higher plasma density. According to Fermat' principle, larger deflection angles are caused by steeper density gradients. As seen from Figure 2-a, a steeper density gradient is related to a higher density of the ablated plasma. Therefore, our modified Nomarski interferometer permits to reach higher plasma density and introduces large errors [26].

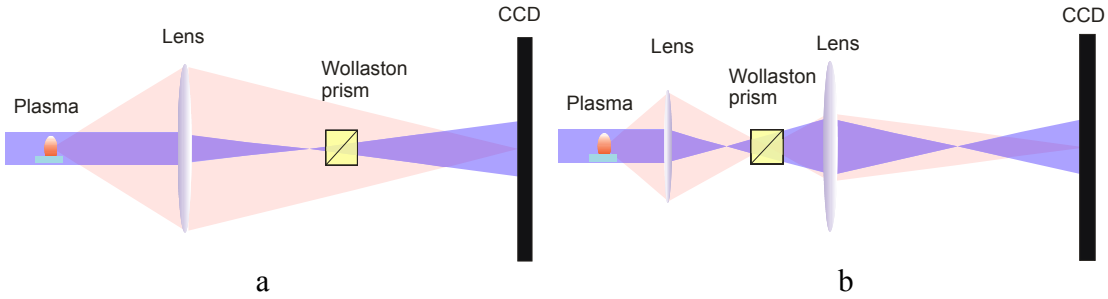

Figure 4. Modification of the interferometer: a). usual Nomarski interferometer; b). presently used interferometer here in this work. The latter one has a lager acceptance solid angle and collects light at a larger deflection angle.

V. Results and analysis

The pump-probe experiment had been repeated for a variety of different time delays (see Figure 2-a) aimed to get a time resolved measurement. Delay times less than 40 ps were not accessible. The six interferograms obtained with a delay time larger than 40 ps are listed in Figure 5. These images have been reconstructed and are listed in Figure 6. These reconstructions were performed by specially developed software for interferometric analysis from Pisa, Italy [27].

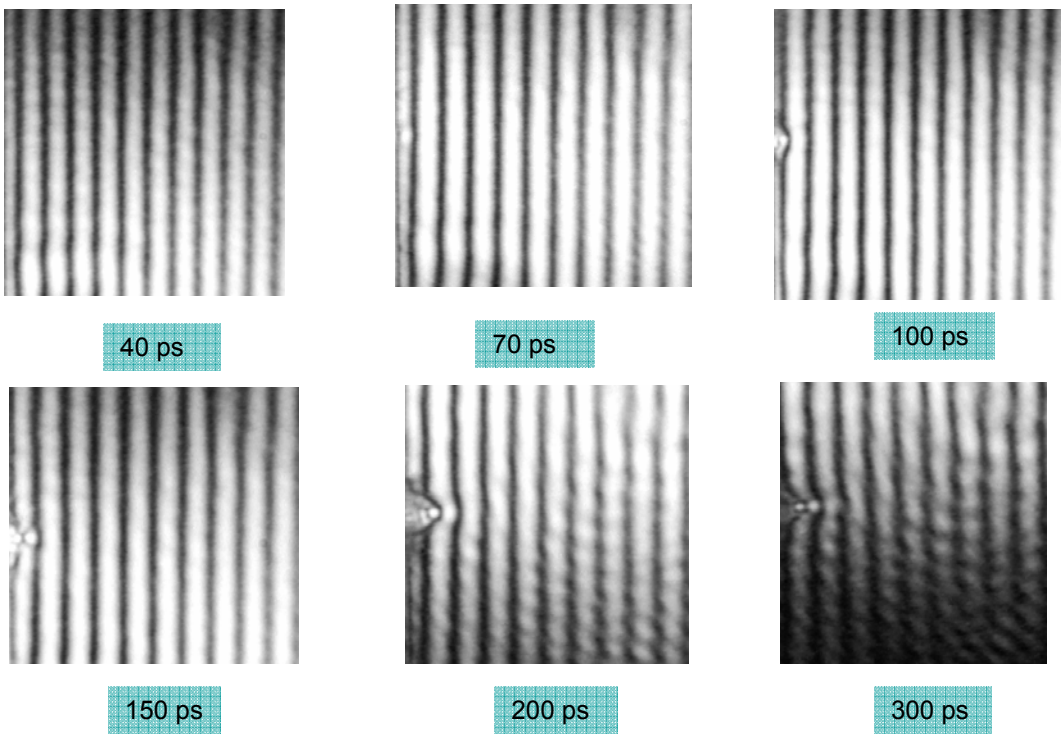

Figure 5. Interfergram obtained in different experiments for different time delay.

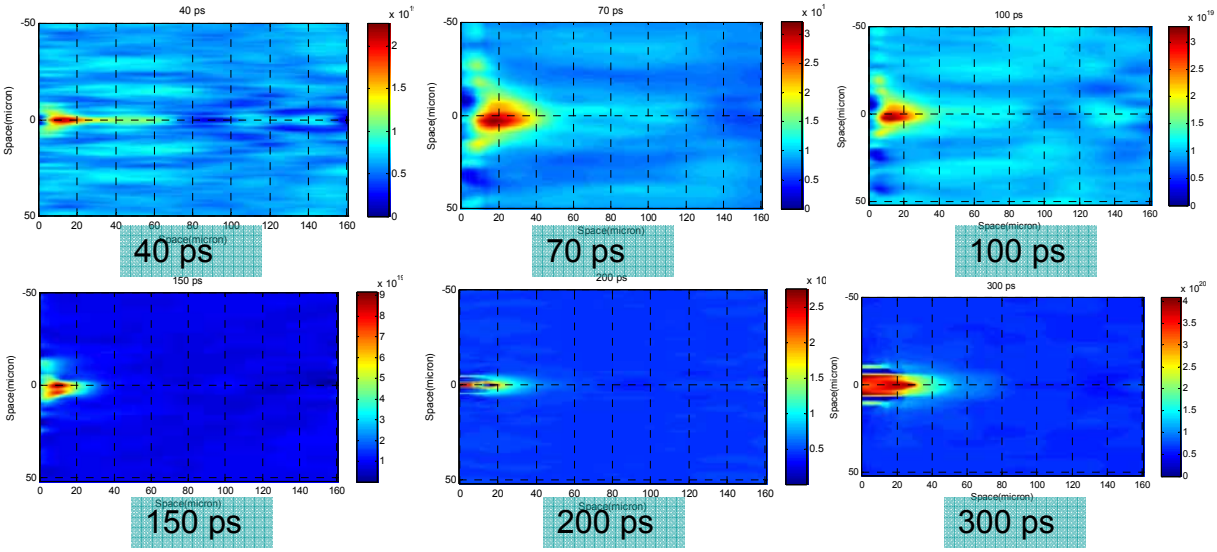

Figure 6. analysis of the interfergram in Figure 5 .

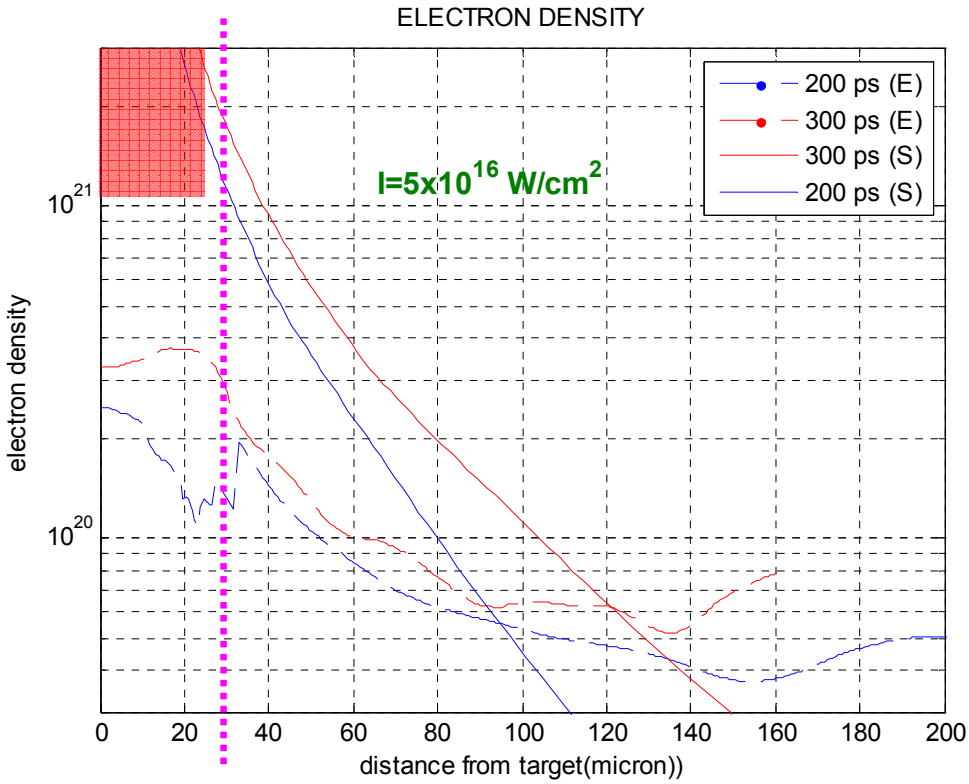

Figure 7. Electron density profiles of the laser-induced along the axis perpendicular to the target. The solid lines give the numerical results while the dashed lines denote the experimental results. The red and the blue lines response to 300 ps and 200 ps time delay respectively.

Figure 7 shows the electron density profiles along the axis perpendicular the target surface. The experimental curves can be divided into two parts in space. The first part is close to the target with a distance of less than 30 μm, the second is further away with a distance larger than 30 μm. The first part close to the surface cannot reflect the density profile of the plasma at that region due to the steep density gradient. In the second part, the measured densities are underestimated because the phase shift of the light traveling through the plasma is reduced due to the deflection into lower density plasma regions. This could explain the discrepancy between the measured and simulated results shown in Figure 7. Minor experimental errors could be attributed to uncertainties of the laser parameters and the determination of the target surface. However, the

measurements in this region can serve as a lower limit for the plasma density. An extrapolation to the density of 10^{21} cm^{-3} would lead to a distance of 25 μm.

VI. Conclusion

Interaction of ultra-short pulse laser and flat PMMA target has been investigated numerically and experimentally. Numerical results show that near-solid density matter at $n_e=10^{21}$-10^{22} cm^{-3} can be found in a region of $z<35$ μm, at the time 300 ps after the pump laser with the parameters 50 fs pulse duration, $5x10^{16}$ cm^{-3} intensity and 800 nm in wavelength. Experimental results show that, the dense matter can be expected in a region of $z<25$ μm, at the time 300 ps after the laser beam pulse (50fs, 3.3J, 10~15μm in focus diameter). According to our results, ablative plasmas can be used as possible targets to probe near solid density matter by Thomson scattering diagnostics using the FLASH FEL. As a main requirement for its application, however, one has to overcome the steep density gradients of the ablated plasma which is possible by using better adopted target surfaces.

VII. Acknowledgement

We gratefully thank Dr. P. Tomassini who provided the software to analysis the interferogram, Mr. U. Zastrau and Ms. H. Marschner who helped to perform the experiments and Dr. K. U. Amthor whose valuable discussions are helpful and important.

This work was performed under the auspices of the **Virtual Institute VH-VI-104** ***Plasma Physics Research Using FEL Radiation*** of the Helmholtz Society, supported by the SFB 652 *Strong Correlations and Collective Phenomena in Radiation Fields: Coulomb Systems, Clusters, and Particles*, LDRD 05-ERI-003, and the Alexander von Humboldt Foundation. Work of O. L. Landen and S. H. Glenzer was performed under the auspices of the U.S. Department of

Energy by University of California LawrenceLiv ermore National Laboratory under contract No. W-7405-Eng-48 and in part under contract DE-AC52-07NA27344.

VIII. Reference

1. R.W. Lee et al., J. Opt. Soc. Am. B**20**, 770 (2003).
2. O.L. Landen et al., J. Quant. Spectrosc. Radiat. Transf. **71**, 465 (2001).
3. E. Nardi et al., Phys. Rev. E**57**, 4693 (1998).
4. D. Riley, et al., Plasma Phys. Control. Fusion **47**, B491 (2005).
5. O.L. Landen et al., Rev. Sci. Instr. **72**, 627 (2001).
6. S.H. Glenzer et al., Phys. Rev. Lett. **17**, 175002-1 (2003).
7. G. Gregori et al., Phys. Rev. E**67**, 026412 (2003).
8. A. Höll, et al., Eur. Phys. J. **D29**, 159-162 (2004).
9. R. Redmer, et al., IEEE Transactions on Plasma Sciences **33**, 77 (2005).
10. R. Thiele et al., J. Phys. A**39**, 4365 (2006).
11. G. Gregori et al., Phys. Rev. E**74**, 026402 (2006).
12. A. Höll, et al., *"Thomson Scattering Measurements of Plasma Dynamics"*, FLASH proposal Sept. 2006.
13. R. Benattar, *et al*, Rev. Sci. Instrum., Vol. 50, 1853 (1979)
14. A. Djaoui, A user guide for the laser-plasma simulation code: MED 103. Rutherford Appleton Laboratory, 1996.
15. T. A. Hall, et at., Phys. Rev. Lett. 81, 1003–1006 (1998)
16. L. LABATE, et al., Laser and Particle Beams, 20, 223–226, (2002)
17. C. Keyser, et al., Appl. Phys. A 77, 217–221 (2003)
18. Hariharan, P., Optical Interferometry, New York: Academic Press, (2003)

19. H. Schittenhelm, et al., Applied. Surface. Science, 1998, Vol. 129, 922 (1998)

20. R. E. Walkup, et al, Appl. Phys. Lett. Vol. 48, 1690 (1986)

21. L. A. Doyle, et al., IEEE transactions on plasma science, Vol. 27, 128 (1999)

22. M. Villagran- Muniz, et al, IEEE transactions on plasma science, Vol. 77 2464 (2000)

23. S. M. Mao, et al, Appl. phys. lett. Vol. 77, 2464 (2000)

24. I. V. lisitsyn, et al, Rev. Sci. Instrum. Vol. 69, 1584 (1998)

25. M. Born and E. Wolf, Principles, Pergamon, Oxford (1964)

26. D. W. Sweeney, et al, Applied Optics Vol.15, 1126 (1976)

27. P. Tomassini, et al, Laser and Particle Beams, Vol. 20, 195 (2002).